J Mater Sci (2006) 41:6492–6496
DOI 10.1007/s10853-006-0756-6

LETTER

The photoconductance of a single CdS nanoribbon

Liu Yingkai · Zhou Xiangping · Hou Dedong · Wu Hui

Received: 19 April 2006 / Accepted: 3 August 2006 / Published online: 21 September 2006

Introduction

Semiconductor nanowires and nanoribbons are being considered as the basis of a variety of device technologies. Recently, ZnO nanowire ultraviolet photodetectors and optical switches have been investigated [1]. The results suggest that they are good candidates for optoelectronic switches. Zhou et al. [2] reported the UV response of SnO_2 nanowires and observed a strong modulation of the conductance in SnO_2 nanowire by UV illumination. CdS is an important semiconductor with a direct band gap of 2.42 eV that falls in the visible region at room temperature. CdS thin films have excellent photoconductive properties and were used in a large number of solid-state device applications such as photoconductive (PC) detection, xerography, photovoltaic solar energy conversion, and thin-film transistor electronics. But up to now, only a relatively small effort has been paid to study the photoconductance of CdS nanoribbons [3] and a single nanowire [4], no one reported the photoconductance of a single CdS nanoribbon. Our objective was to synthesize high-quality CdS nanoribbons, which is a necessary requirement for obtaining fast response optoelectronic device and investigate PC properties of a single CdS nanoribbon.

Experimental and results

CdS nanoribbons with single-crystalline structure were synthesized by thermal evaporation of CdS powders in three-zone furnace [5]. The CdS powders was placed in the middle of zones II, while the silicon substrates coated with 20 Å gold film were placed in the middle of zones II. After the tube was evacuated by a turbomolecular pump to a pressure of 8×10^{-4} Pa, argon was flowed at 15 sccm from zone I to III. The temperatures at the center of the three zones were increased within 30 min to 700, 880, and 400 °C, respectively, and held at these temperatures for 2 h. The pressure was maintained at ~12000 Pa. After the furnace was cooled to room temperature, a yellow wool-like material was deposited on the silicon substrate.

Samples collected from the silicon substrates were characterized by scanning electron microscopy (SEM; Philips XL 30 FEG), and high-resolution transmission electron microscopy (HRTEM; CM200 FEG, operated at 200 kV). Figure 1a is the scanning electron microscope (SEM) images of the synthesized CdS nanoribbons. The width and thickness of the ribbons are in the range of 5–10 μm and 65 nm, respectively. The corresponding high-resolution TEM (HRTEM) image of one CdS nanoribbon is shown in Fig. 2b, revealing the hexagonal structure of CdS. The lattice spacing of 3.54 Å and 6.68 Å corresponds to the (1000) and (0001) crystal planes, respectively. No dislocation and other defects were observed in the CdS nanoribbons,

L. Yingkai (✉) · Z. Xiangping · H. Dedong · W. Hui
Department of Physics, Yunnan Normal University, Kunming, Yunnan, P.R. China
e-mail: liuyingkai99@163.com

L. Yingkai
Center of Super-Diamond and Advanced Films (COSDAF), City University of Hong Kong, Hong Kong SAR, P.R. China

L. Yingkai
Department of Physics and Materials Science, City University of Hong Kong, Hong Kong SAR, P.R. China

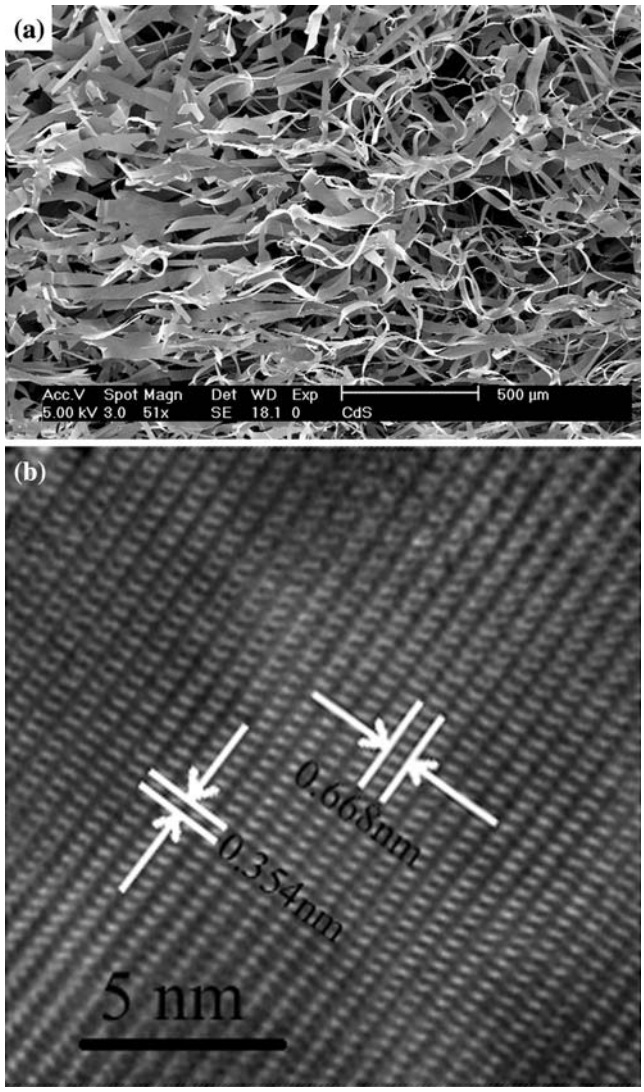

Fig. 1 SEM images of the as-synthesized CdS nanoribbons (**a**) and High-resolution TEM image of one CdS nanoribbon (**b**)

indicating that these nanoribbons are perfect single crystals.

ITO film was grown on the surface of glass and then some isolated gaps (its width was 50 nm) were patterned by lithography. ITO patterns were described as schematically shown in Fig. 2a. The preparation processes were as follows: First, CdS nanoribbons were scratched by tweezers and some products were dispersed in ethanol. Then a few drops of the resulting suspensions were dropped onto an ITO pattern substrate. The CdS nanoribbon flatly lain on the ITO substrate was chosen by optical microscope to measure its photoconductive properties. The surface of ITO is very smooth and ethanol evaporates easily, so the contact of between CdS nanoribbons and ITO is good. Thus the device was obtained. A simulated solar

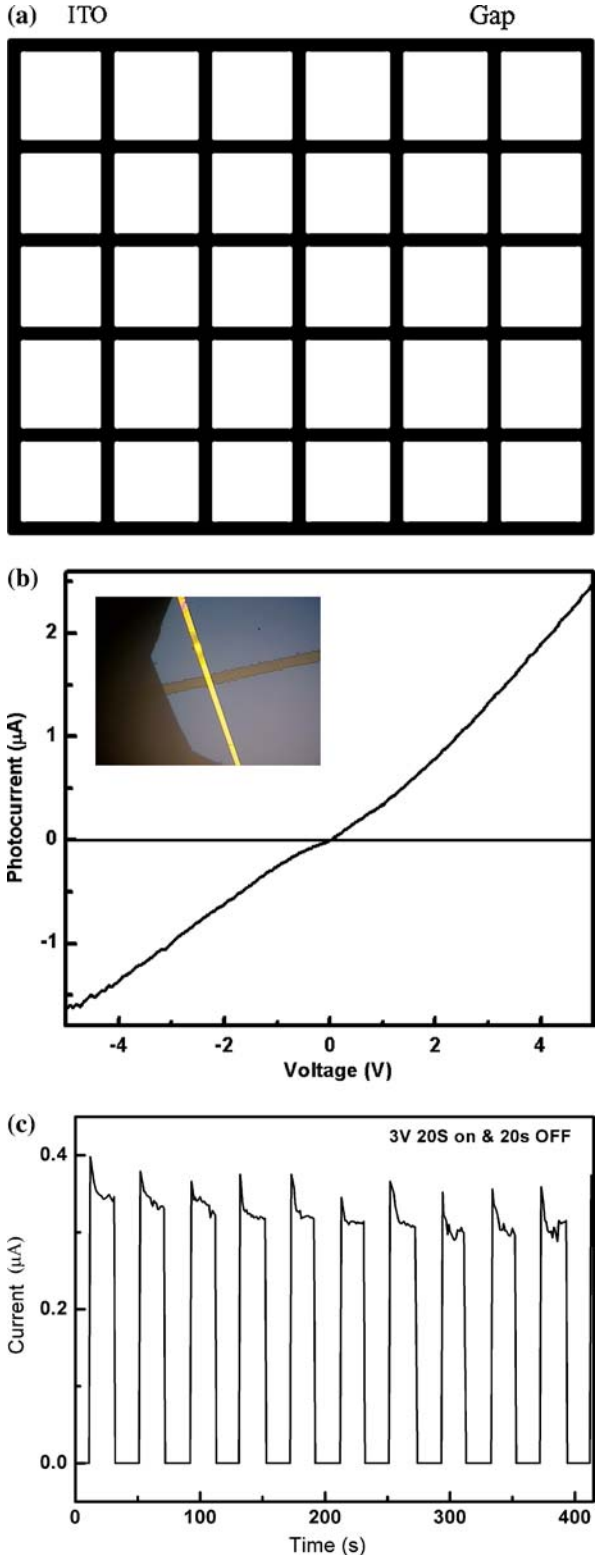

Fig. 2 Schematic illustration of ITO patterns (**a**); *I–V* curves of a single CdS nanoribbon in the dark and under incandescent light illumination, the inset is the measured CdS nanoribbon on the ITO (**b**), and Photocondutance of a single CdS nanoribbon under incandescent light illumination of 2.45 mW/cm^2 with a period of 20 s ON & 20 s OFF (**c**)

radiation has been used as excitation source and a prism monochromator was used for obtaining monochromic light. The photocurrents were measured by a home-built system of City University of HongKong with a digital multimeter. An optical microscope was attached to this system so that the position of CdS nanoribbon was well observed. Applied voltage has been done using a regulated power supply. Due to the low response of our I–V instrument, a resistant is connected to CdS nanoribbon in series so that the photoconductance rise time and decay time of CdS nanoribbon can be measured by the oscilloscope.

Fig. 2b displayed the current–voltage curves of a single CdS nanoribbon recorded in air under an incandescent light illumination intensity of 2.45 mW/cm^2 as well as in dark. Both of the *I–V* curves showed nearly a linear feature, which revealed that the ohmic contact of both CdS nanoribbon and ITO was achieved. The photocurrent in dark was much lower than that under an incandescent light illumination, which indicated that CdS nanoribbon has excellent light response. Inset of Fig. 2b showed the photograph of the measured CdS nanoribbon on the ITO (the width of gap was 50 nm). The width of CdS nanoribbon was 25 nm.

Fig. 2c showed the current measured over time of a single CdS nanoribbon at a constant $V = 3$ V, and the photoconductance modulation were induced by turning a shutter for the incandescent light ON and OFF 10 times. The used incandescent light intensity was 2.45 mW/cm^2. The duration of ON and OFF time was 20 s. The current was observed to increase dramatically and stabilize at high-conductance ''ON'' state under incandescent light illumination; whereas it decreased quickly and landed at a low-conductance ''OFF'' state after the incandescent light was blocked. The photocurrent was from ~1.1 pA to 7.5 μA, i.e. the current density is from 8.5×10^{-2} to 2.8×10^5 A/cm^2, which exhibited good switch properties. The relative photosensitivity factor *S*, defined by

$$S = \Delta\sigma/\sigma_d = (R_d - R_i)/R_i$$

where R_d and R_i represent dark resistance and resistance under illumination. In single CdS nanoribbon the value of *S* is found to be as high as 10^5 under the incandescent light illumination intensity of 2.45 mW/cm^2. Therefore, one nanoribbon can be used as one switch. In addition, we also checked the reliability of CdS nanoribbon and found that it was stored in air after two months; its photoconductance did not decrease.

For comparison, we study the effect of different wavelength on CdS nanoribbon, many monochromic light are obtained from simulated solar by monochromator. Figure 3a is *I–V* curves of a single nanoribbon under different wavelength light illumination, which is normalized by $I_{PC} \propto P^{0.8}$ (I_{PC} is photocurrent, *P* is the power density of illumination) [6]. The *I–V*

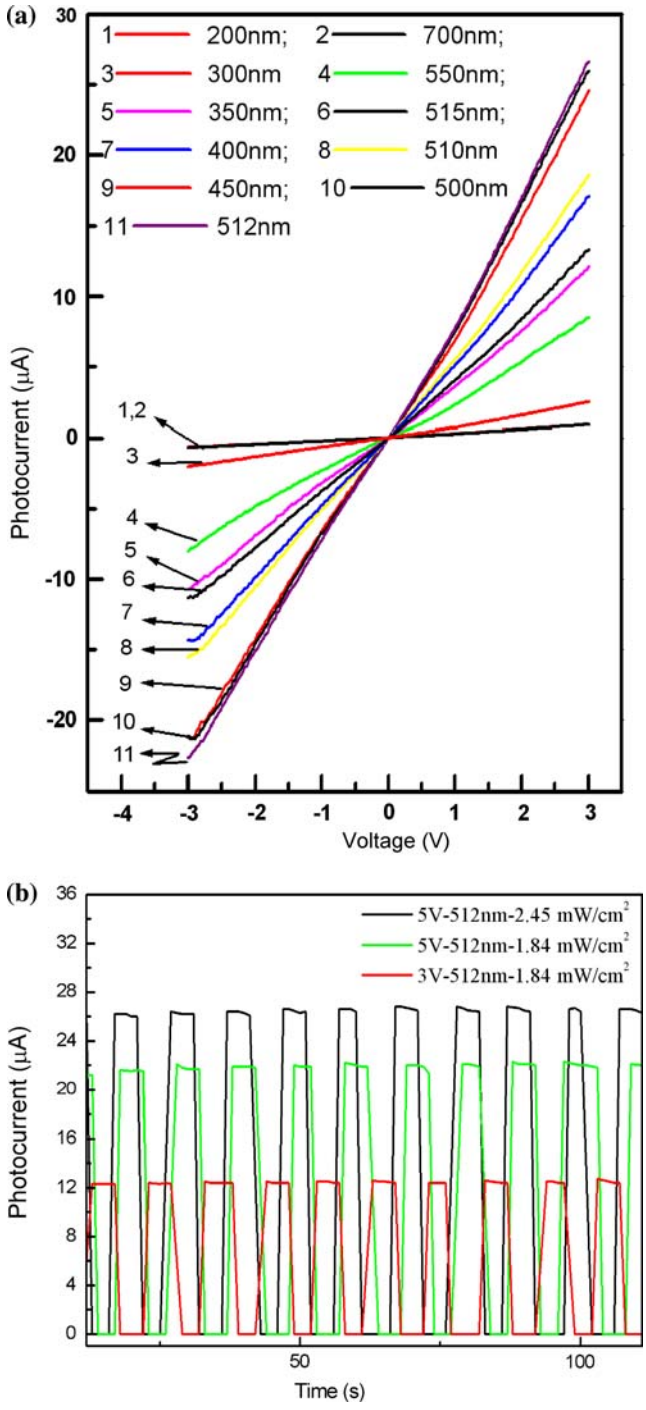

Fig. 3 *I–V* curves of a single CdS nanoribbon of different wavelength light obtained from simulated solar irradiation by monochromator (**a**), and photoconductance comparison of 512 nm light under different powder density and applied voltage (**b**)

characteristics have been found to be nearly linear within the voltage range of study. It is also found that photoconductance of a single CdS nanoribbon under different wavelength light illumination are different and among them the photoconductance under 512 nm monochromatic light is the largest. In addition, the current-time of a single CdS nanoribbon at constant V = 3 V and 5 V is measured, as shown in Fig. 3b, and the photoconductance modulation are induced by turning a shutter for the 512 nm light ON and OFF 10 times. The used intensities of light illumination are 2.45 and 1.84 mW/cm^2, respectively and the results are also shown in Fig. 3b. This figure shows that the behavior of photocurrent with time at different intensity and different applied voltage is similar to that in Fig. 2c. The value of S is up to 10^7 and the highest current density is up to 2.1×10^6 A/cm^2. Compared to those under incandescent light, the value of S is enhanced by two orders. The reason will be analyzed in the following paragraph.

We further analyze the current–time behaviors of the CdS nanoribbon and find that under the same illumination intensity the ratio of the photocurrent magnitude at 5 V to that at 3 V is 1.72, showing a nearly linear dependence on the applied voltage because the ratio of 5 V to 3 V equals to 1.67. At the same applied voltage, the ratio of the photocurrent magnitude under the illumination intensity of 2.45 mW/cm^2 to that under illumination intensity of 1.84 mW/cm^2 is 1.21. It almost satisfies the relationship of $I_{PC} \propto P^{0.8}$ [6], which indicated that the photoconductance was related to electron-hole generation, trapping, and recombination within the semiconductor.We also noticed that the I–V relationship of Fig. 2b and 3a is not linear over the whole applied voltage range covered and that the lines are not straight and there are some noises on them at high-conductance ''ON'' state of Fig. 2c and 3b. It may be due to the temperature fluctuation and the difference of illumination intensity induced by the applied voltage fluctuation. Based on our experiment the latter is main factor led to the above-mentioned results.

Figure 4 is the voltage rise and decay edge of a resistant, which is measured by the oscilloscope. It reflects the photoconductance rise time and decay time of CdS nanoribbon. With and without 512 nm light illumination intensity of 2.45 mW/cm^2, the voltage of the resistant changes from 0 to 4 V. It is seen that the transient time of ''ON'' and ''OFF'' state is very sharp and easily measured that the rise and decay time are 551 μs and 1.093 ms, respectively. The values are faster than those of bulk CdS single crystal and film [3, 7–9]. If the used light illumination intensity is increased, the rise and decay time will further become shorter. The reason of the rise and decay time measured by the oscilloscope is that it is impossible to well and truly measure the rise and decay time of CdS nanoribbon from I–V curves of CdS nanoribbon (Figs. 2c and 3b) because of the slow response of our I–V measurement instrument.

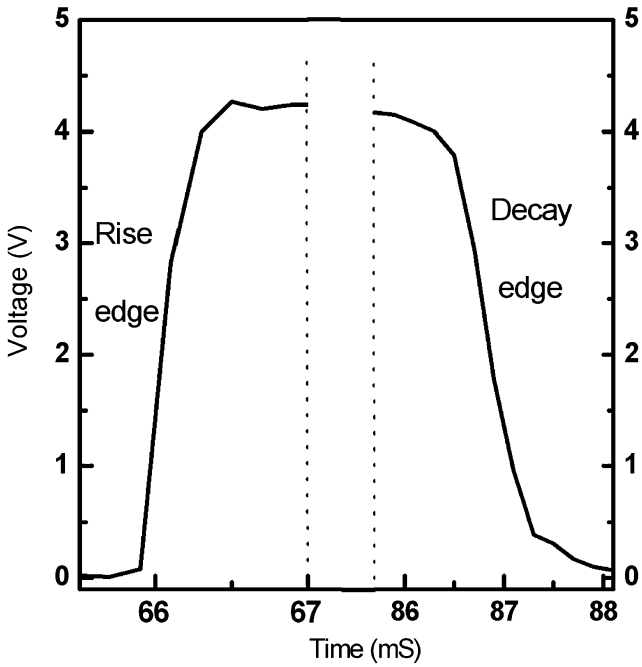

Fig. 4 The voltage rise and decay edge of a resistant under 512 nm light illumination intensity of 2.45 mW/cm^2

Compared to other results of CdS belts and film [3, 7–9], not only have we measured the photoconductance of a single CdS nanoribbon but also the photo-to-dark conductance ratio, i.e. S was the highest, whereas the used illumination intensity is much smaller than that of their experiments [3, 7–9]. More importantly, the rise time and decay time were the shortest. This is very important in fabricating optoelectronic switches, light amplifiers, and counting circuits.

As to the photoconductance mechanism, it is generally accepted that the photoconductance in the CdS films is mainly ascribed to photogenerated electrons, the adsorption and desorption of the chemisorbed oxygen on the surface of CdS [10]. N-type CdS films are especially susceptible to O_2 adsorption effect [11–13]. If there are some effects on the CdS nanoribbon, physically adsorbed O_2 can take an electron from material to form a chemically adsorbed surface state.Photoconductance σ_{ph} can be expressed as this formula [14]

$$\sigma_{ph} = eG\mu_n\tau_n \quad (1)$$

where σ_{ph} is the photoconductance; e is the electronic charge, G is the photocarrier generation rate, and μ_n is the electron mobility, τ_n is the free lifetime of the photogenerated electrons. Based on these, the photoconductance mechanism of CdS nanoribbon can be described as follows: Upon light illumination, on the one hand the photocarriers are generated, accordingly G increased. Simultaneously, the electron mobility of CdS nanoribbon is also increased. For CdS, the electron Hall mobility upon illumination has been detected to increase two orders of magnitude [15] and the electron mobility is up to 340 $cm^2 V^{-1} s^{-1}$ [16]. On the other hand CdS nanoribbon is very thin and almost has no microstructure defects in it. However, O_2^- and O^- adsorb on the surface of the nanoribbon and lead to the formation of barriers at the adsorbate sites. The absorbed oxygen is subsequently released due to light illumination, which reduces the barrier height, thereby promoting the electron transport. Therefore the photoconductance of CdS nanoribbon under illumination is increased by many orders. Thus, the photoconductance of CdS nanoribbon is larger than that of its counterpart films whereas the rise time and decay time are shorter than those of CdS films. We may explain these results as this: for CdS films [7–9], they contained impurities and then these impurities created defect states, which may act as recombination centers and traps. The recombination process reduced the lifetime of the charged carriers in the conduction or valence band, and therefore the photoconductance is reduced [17], whereas the traps retain electrons for a considerable time and hence the rise time and decay time of photoconductance became slow. In addition, CdS nanoribbons are perfect single crystals. These crystals may have a decisive role in the characteristics and may be partly responsible for the peculiar photoconductance. This may be revealed in a more thorough investigation.

Now, we may return to explain the other experimental phenomena. Exposure of CdS nanoribbons to irradiation at 512 nm wavelength would typically correspond to the highest photoconductivity due to an interband charge carrier generation [18]. It is assumed that the largest photoconductive component under 512 nm light illumination (Fig. 3) is related to the interband excitations in the CdS nanoribbon. Therefore, the photoconductance of the CdS nanoribbon under 512 nm light illumination is much improved. Studies of other factors leading to high photoconductance and improving photoconductance are underway.

Conclusions

In summary, photoconductance of a single CdS nanoribbon was measured under an incandescent light illumination and 512 nm light illumination by using ITO as electrodes. For CdS single crystal nanoribbon, ITO is a good electrode. It is also found that the photo-to-dark conductance ratios of a single CdS nanoribbon were 10^5 and 10^7 under incandescent light illumination and 512 nm light irradiation. The photoconductance rise and decay time of CdS nanoribbon under 512 nm light illumination are 551 μs and 1.093 ms, respectively. The high photoconductance, the short rise time and decay time are very important for CdS nanoribbon used in the field of optoelectron and other fields.

Acknowledgements The work was supported by a grant from Natural Science Foundation of Educational Council of Yunnan Province (No. 5Z0098A) and the Research Grants Council of the Hong Kong SAR, China [No. CityU 3/01C (8730016)], a Strategic Research Grant of Hong Kong University [No. 7001175].

References

1. Kind H, Yan HQ, Messer B, Law M, Yang PD (2002) Adv Mater 14:185
2. Liu ZQ, Zhang DH, Han S, Li C, Tang T, Jin W, Liu XL, Lei B, Zhou CW (2002) Adv Mater 15:1754
3. Li QH, Gao T, Wang TH (2005) Appl Phys Lett 86:193109
4. Gu Y Kwak ES, Lensch JL, Allen JE, Odom TW, Lauhon LJ (2005) Appl Phys Lett 87:043111
5. Liu YK, Zapien JA, Shan YY, Geng CY, Lee CS, Lee ST (2005) Adv Mater 17:1372
6. Rose A (1978) Concepts in photoconductivity and allied problems. Krieger
7. Publishing Company, New York
8. Fu SL, Wu TS, Houng MP (1985) Sol Energy Mater 12:309
9. Porada Z, Shabowska E (1980) Thin Sol Films 66:455
10. Tschulena G Battelle Institutes, Frankfurt, Private Communications
11. Amalnerkar DP (1999) Mater Chem Phys 60:1
12. Shear H, Hilton EA, Bube RH (1965) J Electrochem Soc 112:997
13. Robinson AL, Bube RH (1965) J Electrochem Soc 112:1001
14. Bube RH (1966) J Electochem Soc 113:793
15. Nair PK, Nair MTS, Campos J, Sansores LE (1987) Sol Cells 22:211
16. Wu CH, Bube RH (1974) J Appl Phys 45:648
17. Sze SM (1981) Physics of semiconductor devices. Interscience, New York, p 849
18. Joson NV (1990) Photoconductivity: art, science, and technology. Marcel Dekker, Inc., New York and Basel p 49
19. Bube RH (1992)Photoelectronic properties of semiconductors. Cambridge University Press, Cambridge